Advances in Adaptive Data Analysis
Vol. 3, No. 4 (2011) 509–526

DOI: 10.1142/S1793536911000891

World Scientific
www.worldscientific.com

WEIGHTED SLIDING EMPIRICAL MODE DECOMPOSITION

R. FALTERMEIER*
Department of Neurosurgery,
University Hospital Regensburg,
93040 Regensburg, Germany
rupert.faltermeier@klinik.uni-regensburg.de

A. ZEILER
CIML Group, Biophysics Department,
University of Regensburg,
93040 Regensburg, Germany
angela.zeiler@biologie.uni-regensburg.de

A. M. TOMÉ
IEETA/DETI, Universidade de Aveiro,
3810-193 Aveiro, Portugal
ana@ieeta.pt

A. BRAWANSKI
Department of Neurosurgery,
University Hospital Regensburg,
93040 Regensburg, Germany
alexander.brawanski@klinik.uni-regensburg.de

E. W. LANG
CIML Group, Biophysics Department,
University of Regensburg,
93040 Regensburg, Germany
elmar.lang@biologie.uni-regensburg.de

The analysis of nonlinear and nonstationary time series is still a challenge, as most classical time series analysis techniques are restricted to data that is, at least, stationary. Empirical mode decomposition (EMD) in combination with a Hilbert spectral transform, together called Hilbert-Huang transform (HHT), alleviates this problem in a purely data-driven manner. EMD adaptively and locally decomposes such time series into a sum of oscillatory modes, called Intrinsic mode functions (IMF) and a nonstationary component called residuum. In this contribution, we propose an EMD-based method, called Sliding empirical mode decomposition (SEMD), which, with a reasonable computational effort, extends the application area of EMD to a true on-line analysis

*Corresponding author.

of time series comprising a huge amount of data if recorded with a high sampling rate. Using nonlinear and nonstationary toy data, we demonstrate the good performance of the proposed algorithm. We also show that the new method extracts component signals that fulfill all criteria of an IMF very well and that it exhibits excellent reconstruction quality. The method itself will be refined further by a weighted version, called weighted sliding empirical mode decomposition (wSEMD), which reduces the computational effort even more while preserving the reconstruction quality.

Keywords: Empirical mode decomposition (EMD); weighted sliding empirical mode decomposition (wSEMD); on-line EMD; sliding intrinsic mode functions.

1. Introduction

In 1998, an empirical nonlinear analysis tool for complex and nonstationary time series has been pioneered by Huang *et al.* [1998]. It is commonly referred to as empirical mode decomposition (EMD) and, if combined with Hilbert spectral analysis, it is called Hilbert-Huang transform (HHT). It adaptively and locally decomposes any nonstationary time series in a sum of intrinsic mode functions (IMF), which represent zero-mean amplitude and frequency-modulated oscillations. EMD provides a fully data-driven and unsupervised signal decomposition, and does not need any *a priori* defined basis system. EMD also satisfies the perfect reconstruction property, i.e. superimposing all extracted IMFs together with the residual slow trend reconstructs the original signal without information loss or distortion. The method is thus similar to the traditional Fourier or wavelet decompositions, but the interpretation of IMFs is not similarly transparent in the sense that IMFs do not always represent physically meaningful and observable modes. In the paper by Jánosi and Müller [2005], for example, it was observed that their extracted IMFs did not correspond to seasonal components of the ozone time series under study. Hence, it appears being a challenging task to identify and/or combine extracted IMFs in a proper way to yield physically or physiologically meaningful characteristic modes of the system under study. However, the empirical nature of EMD offers the advantage over other empirical signal decomposition techniques such as empirical matrix factorization (EMF) of not being constrained by conditions that often only apply approximately. In daily practice, for example, in medical facilities, time series are recorded over long time periods and often with high sampling rates; therefore, a huge amount of data is collected. Existing EMD algorithms then reveal two shortcomings. First, the analysis of such data has to wait until data collection is finished. Second, the huge amount of data does not allow its complete analysis, rather the recorded time series are segmented to render them tractable by current EMD techniques and available computational capacities. These shortcomings generate the need for a truly *on-line* variant of EMD algorithms which is able to analyze recorded data in real time. This contribution will shortly review the technique of EMD and its recent extensions. The latter include a suggestion of an *on-line* EMD algorithm [Rilling *et al.* (2003)] which, however, is neither robust nor efficient. Such an algorithm, called sliding empirical mode decomposition (SEMD)

[Faltermeier *et al.* (2010)], and its extension called weighted SEMD (wSEMD) is proposed here, and its properties and applications to large-scale time series data is discussed.

2. Empirical Mode Decomposition

The EMD method was developed from the assumption that any nonstationary and nonlinear time series consist of different simple intrinsic modes of oscillation. The essence of the method is to empirically identify these intrinsic oscillatory modes by their characteristic time scales in the data, and then decompose the data accordingly. Through a process called *sifting*, most of the *riding waves*, i.e. oscillations with no zero crossing between extrema, can be eliminated. The EMD algorithm thus considers signal oscillations at a very local level and separates the data into locally nonoverlapping time scale components. It breaks down a signal $x(t)$ into its component IMFs obeying two properties:

(1) An IMF has only one extremum between two subsequent zero crossings, i.e. the number of local minima and maxima differs at most by one.
(2) The local average of the upper and lower envelopes of an IMF has to be zero.

Note that the second condition implies that an IMF is stationary that simplifies its analysis. However, an IMF may have amplitude modulation and also changing frequency.

2.1. *The standard EMD algorithm*

The sifting process can be summarized in the following algorithm. Decompose a data set $x(t)$ into IMFs $x_n(t)$ and a residuum $r(t)$ such that the signal can be represented as

$$x(t) = \sum_n x_n(t) + r(t). \tag{1}$$

The complete procedure of decomposing a time series via EMD is illustrated schematically in Fig. 1.

The average period of each IMF can be calculated by dividing twice the sample size $2 \cdot N$ by the number of zero crossings. Note also that the number of IMFs extracted from a time series is roughly equal to $ld(N) := \log_2(N)$. The sifting process separates the nonstationary time series data into locally nonoverlapping IMFs. However, EMD is not a sub-band filtering technique with predefined waveforms such as wavelets. Rather, the selection of modes corresponds to an automatic and adaptive time-variant filtering. The completeness of the decomposition process is automatically achieved by the algorithm as $x(t) = \sum_{n=1}^{i} x_n(t) + r(t)$ represents an identity. Further, the EMD algorithm produces *locally orthogonal* IMFs. Global

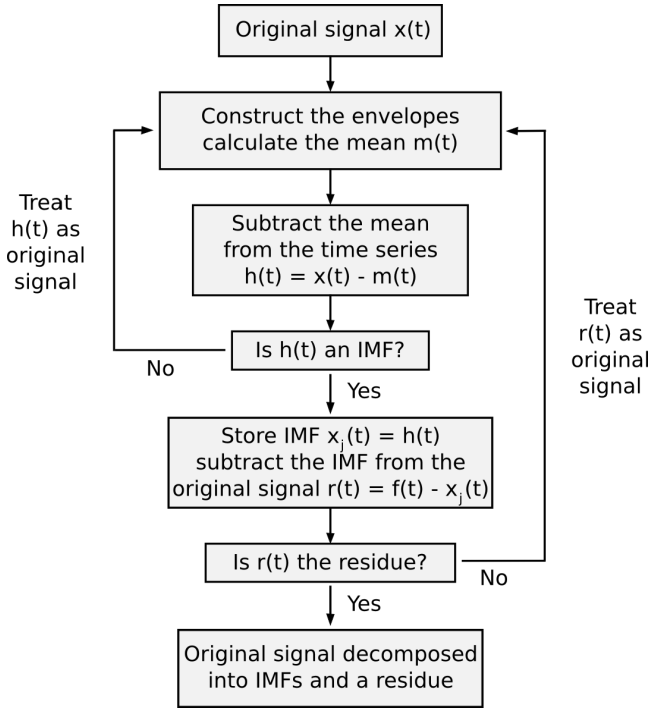

Fig. 1. Flowchart describing the principle mode of operation of EMD.

orthogonality is not guaranteed as neighboring IMFs might have identical frequencies at different time points (typically in <1% of the cases [Huang *et al.* (1998)].

2.2. *Recent extensions of the standard EMD*

A number of extensions to plain EMD have been proposed in recent years such as

- Ensemble EMD (EEMD) that is a noise-assisted method to improve sifting [Wu and Huang (2009); Flandrin *et al.* (2005)]. In practice, EEMD works as follows:
  (a) Deliberately add white noise to the data set.
  (b) Decompose the noisy data into IMFs.
  (c) Iterate these steps and at each iteration add white noise.
  (d) Calculate an ensemble average of the respective IMFs to yield the final result.
- *Local EMD* [Rilling *et al.* (2003)] that pursues the idea to iterate the sifting process only in regions where the mean is still finite to finally meet the stopping criterion everywhere. Localization can be implemented via a weighting function $w(t)$, which is $w(t) = 1$ in regions where sifting is still necessary and decays to zero at the boundaries. This can be easily integrated into the EMD algorithm via

$$h_{j,n}(t) = h_{j,n-1}(t) - w_{j,n}(t)m_{j,n}(t). \tag{2}$$

This procedure essentially improves the sifting process and tries to avoid *over-sifting*.

- *On-line EMD*: The application of EMD to biomedical time series is limited by the size of the working memory of the computer. Hence, in practical applications, only relatively short time series can be studied. However, many practical situations such as continuous patient monitoring ask for an *on-line* processing of the recorded data. Recently, a blockwise processing, called *on-line EMD*, has been proposed [Rilling *et al.* (2003)]. The method is still in its infancy and needs yet to be developed into a robust and efficient *on-line* technique.

3. Sliding EMD

Plain EMD is applied to the full length signal that in view of limited resources such as computer memory also limits the length of the time series to be dealt with. This, for example, is an especially serious problem in dealing with biomedical time series, which often are recorded over very long time spans with high sampling rates. Analyzing such large data sets all at once is hardly possible because of the computational load involved when using conventional EMD. Even more important, however, is the fact that data analysis has to wait until monitoring is finished. Hence, an immediate *on-line* analysis of such time series data is of utmost importance. One possible solution would be to cut the data into several distinct pieces and apply EMD to this segments. However, in this case, due to the well-known boundary problem of EMD, discontinuities will occur as depicted in Fig. 2. No proper

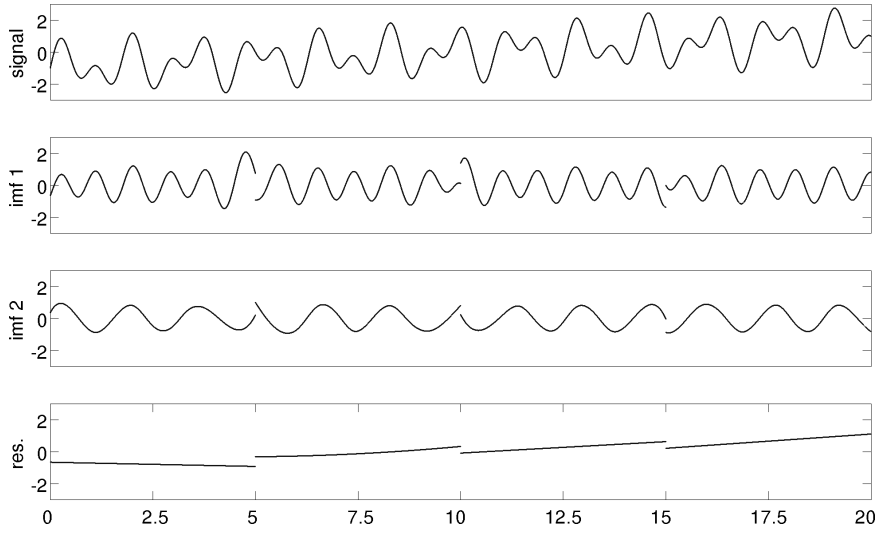

Fig. 2. EMD decomposition of a toy signal. The time series has been segmented into four segments and decomposed with EMD. After joining the resulting IMFs together, boundary effects become clearly visible at $t = 5, 10$ and $t = 15$.

EMD algorithm is available yet that solves these problems and yields reasonable results. In the following section, we will propose a just in time version of EMD called or SEMD. This algorithm will decompose time series of arbitrary length into a residuum and a particular number of IMF-like functions called sliding intrinsic mode functions (SIMFs). In subsequent paragraphs, we discuss the operating mode of SEMD and some characteristics of the SIMFs and the (sliding) residuum. We focus on the well-known boundary effects during EMD and on the reconstruction quality of SEMD. We then use toy data to analyze the reconstruction quality of the sliding residuum and the SIMFs for different parameter settings.

3.1. *The principle of SEMD*

To decompose a time series of arbitrary length with SEMD, a fixed window size m and a step size k have to be chosen. Within such a window, a traditional EMD or EEMD will be performed. Next, the window is shifted by k samples and an EMD is applied again. The resulting SIMFs and residua are combined in a proper way, and the whole process is repeated incessantly. Due to the above-mentioned boundary problems of EMD, the step size k should be chosen much smaller than m, as discontinuities would occur otherwise (see Fig. 2).

If $k < m$ and, in addition, the window size is a multiple of the step size, i.e. if

$$E = \frac{m}{k} \in \mathcal{N} \tag{3}$$

holds, then for each sample $x(t)$ of the original time series, E estimates are calculated within the different windows m_i, as soon as the first E iterations have been done. Due to the above-mentioned boundary problems of EMD, the estimates E_i for a distinct sample $x(t)$ may vary. Bearing EEMD in mind, the mean value of all estimates $x(t)$ is taken as the resulting value of SEMD for this sample. Figure 3 illustrates the principle mode of function of the SEMD algorithm schematically.

The time series in every segment m_i is decomposed by EMD into j eventually different IMFs $x_{m_i j}(t)$ and a local residuum $r_{m_i}(t)$ according to

$$x_{m_i}(t) = \sum_j x_{m_i j}(t) + r_{m_i}(t), \tag{4}$$

whereby the number of sifting steps is kept equal in all segments. Resulting IMFs are collected in a matrix with corresponding sample points, i.e. the different estimates of every sample form a column of the matrix with E entries. Columns corresponding to the beginning or end of the time series are deficient; hence, they are omitted from further processing. This assures that all columns contain an identical amount of information for estimating average IMF amplitudes at every time point t in each segment. This finally yields for $t > m$:

$$x_j(t) = \frac{1}{E} \sum_i^{i+E-1} x_{m_i j}(t), \tag{5}$$

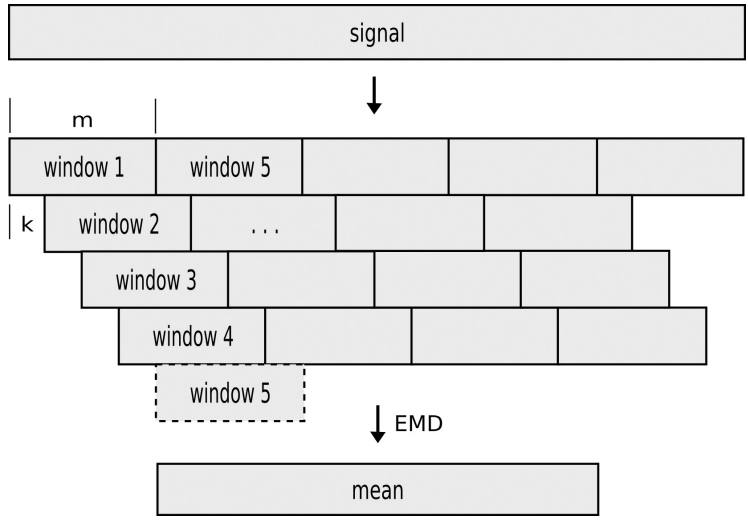

Fig. 3. Schema of the SEMD algorithm. The time series segments in the shifted windows are EEMD. IMFs and the residuum are determined finally by mode amplitudes which are averaged over corresponding samples in all windows. m describes the window size and k the step size.

$$r(t) = \frac{1}{E} \sum_{i}^{i+E-1} r_{m_i}(t), \tag{6}$$

$$i = \left\lfloor \frac{t-m}{k} \right\rfloor + 2. \tag{7}$$

According to traditional EMD, the resulting functions $x_j(t)$ are called SIMFs and $r(t)$ the sliding residuum, respectively. Equations (5)–(7) comprehend the completeness of the SEMD decomposition process. For every sample $x(t)$, the mean value of the E decompositions, done by conventional EMD, forms the result of the SEMD decomposition. As all of these EMD decompositions are complete, so this holds also for the mean value. Problems would arise if the number of IMFs would change for different windows. Therefore, the number of sifting steps and IMFs is kept constant for all decompositions.

3.1.1. *Weighted estimates*

The boundary artifacts of classical EMD affect reconstruction quality primarily at both ends of the original data set, whereat the penetration depth of these artifacts usually grows for higher IMFs (Fig. 4). When using SEMD, this influence will be diminished by computing the mean value of the E estimates. Nevertheless, estimates stemming from the boundaries are expected to be more defective as the ones resulting from the middle part of any specific window. To accommodate SEMD to this fact, a weighted sum of the estimates will be employed that reduces the influence of estimates originating from the border of a window. To accomplish this,

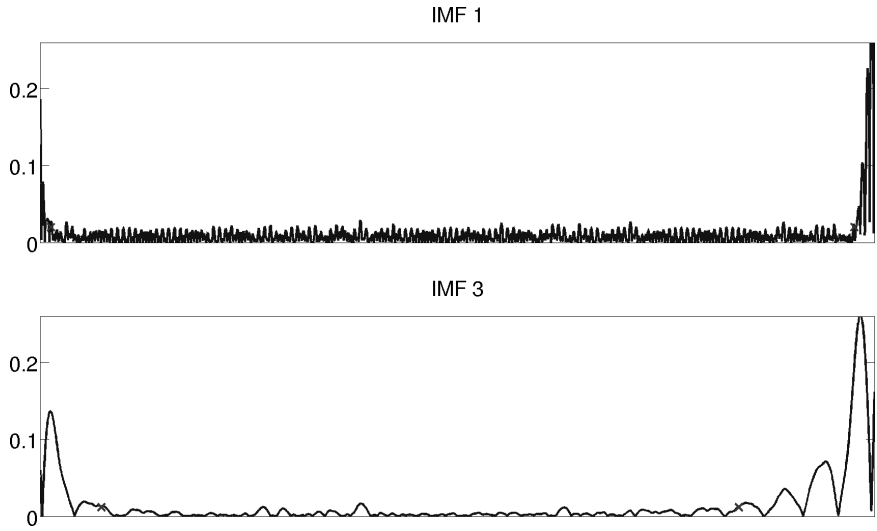

Fig. 4. The time series depicts the reconstruction error of IMF 1 and IMF 3 after EMD was applied to a window of size $m = 2,500$. As input signal toy data (Fig. 5) were used.

for every window, the resulting IMFs and residua are multiplied by a vector of rank m,

$$w(n) = \exp\left(-\frac{1}{2}\left(\alpha\frac{2n}{N}\right)^2\right), \tag{8}$$

$$-\frac{N}{2} \leq n \leq \frac{N}{2}, \quad \alpha = 2.5, \quad N = m - 1, \tag{9}$$

generated from a Gaussian distribution. To calculate a data point of an arbitrary IMF, first the sum over n estimates multiplied by n weighting coefficients is calculated. Then, the resulting value is normalized by the reciprocal of the sum of all used weights again. Hence, the amplitude of every SIMF and the sliding residuum is preserved and the completeness of the decomposition is obtained again. In the following, we will explicitly call the method wSEMD if the above-described weighting is used and compare it to SEMD, EEMD, or EMD.

3.2. *Properties of SEMD and wSEMD*

Contrary to global EMD, the local residua estimated with SEMD for every segment may turn into low-frequency oscillations when joined together into an average global sliding residuum. By choosing the segment size properly, it may be determined which oscillations should appear as distinct SIMF and which should be absorbed as apparent local trends into the respective residua. These apparent local trends may combine into low-frequency oscillations in the final average global sliding residuum. The latter is emerging from an on-line analysis and can be down-sampled employing

an appropriate time step. A subsequent SEMD analysis should apply a window size appropriate for extracting the slow oscillations of the previously re-sampled time series. This process can be repeated until finally a truly monotonous trend remains. Hence, this cascaded application of SEMD acts like a low-frequency filter revealing long-term oscillations and trends that are typically observed in biomedical time series.

Similar to EEMD, also with SEMD an averaging over differently decomposed data sets is achieved. While with EEMD, due to added noise, a given sample is associated with different amplitudes, with SEMD, instead, the same amplitude is associated with different samples in different shifted segments. This latter behavior alleviates the effects related with a nonunique data decomposition via EMD. Furthermore, the artifacts resulting from end effects are suppressed via averaging. Finally, segmentation with proper window size and step size does not result in boundary artifacts after combining local IMFs. SEMD is furthermore similar to *local EMD* in that the stopping criterion needs to be valid only locally, i.e. within the window considered. This substantially reduces *oversifting* and drastically limits the number of necessary sifting steps until the stopping criterion is met locally. Finally, note that while local IMFs fulfill all defining conditions, this is not necessarily true for the resulting average SIMFs though the related deviations are expected to be always small. To take a closer look to the properties of SEMD, we will use a toy signal (see Fig. 5) consisting of a sawtooth wave $(1.5708)^{-1}\arcsin(\sin(699\,x))$, a sinusoid $\sin(327\,x)$, a cosine function with a time-dependent frequency $\cos(2\cdot(x+20)^2)$, and a monotonic trend $0.1\,x-1$, which renders the superimposed signal nonstationary. The oscillatory components are chosen carefully regarding their frequency, so that mode mixing does not occur. For the time series $40,000$, data points were used with $\Delta x = 0.0005$.

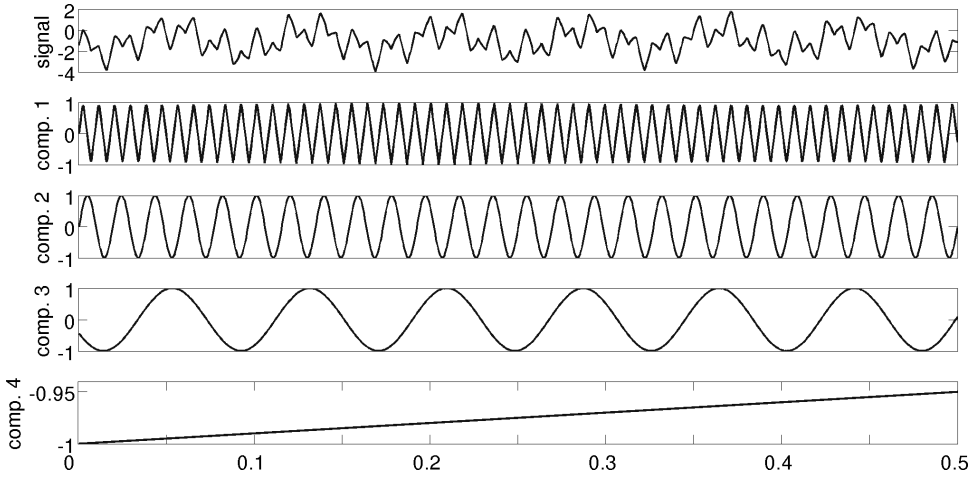

Fig. 5. A detail of the toy signal (top trace) consisting of a sawtooth wave, a sinusoid, a cosine function with time-dependent frequency, and a monotonic function (lower traces).

3.2.1. *Examination of the IMF criteria*

Due to the combination of different parts from different IMFs for the construction of an SIMF, it has to be verified if they obey the conditions to be fulfilled by an IMF. First, the local average $m(t)$ of the upper and lower envelopes (see Fig. 1) of an IMF has to be zero. Second, the number of local extrema and zero crossings can differ by one at most. Evaluating the results, one has to keep in mind that the number of sifting steps is kept constant in the algorithm, so that SEMD, weighted SEMD, and also EEMD work properly (see Sec. 3.1). This method was first introduced by Wu and Huang (2004), which means that also for plain EMD the stopping criterion respectively the IMF criteria are not necessarily fulfilled.

3.2.2. *Mean value*

Figures 6 and 7 show the mean of the absolute values of $m(t)$ for SIMF 1 and SIMF 3 of the toy data with respect to different ensemble sizes. For comparison, the same results are shown for IMF 1 and IMF 3 of a corresponding EMD or EEMD analysis.

For SIMF 1, both SEMD and, especially, wSEMD produce a decomposition that meets the first criterion as good as plain EMD as soon as an ensemble size of *ca.*

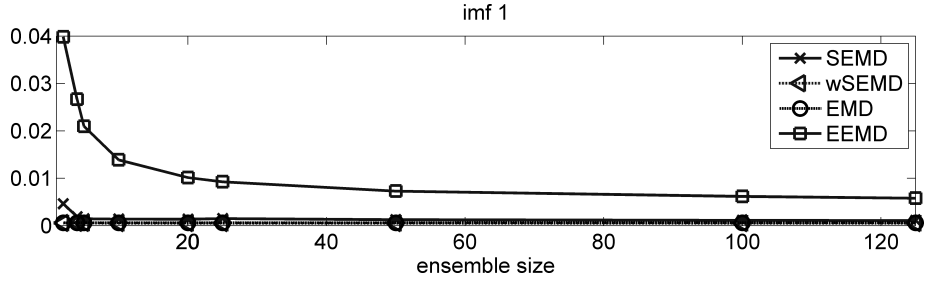

Fig. 6. Evolution of the mean of the absolute values of $m(t)$ for SIMF/IMF 1 obtained with SEMD, weighted SEMD, EMD, and EEMD of the toy data with respect to the ensemble size is depicted.

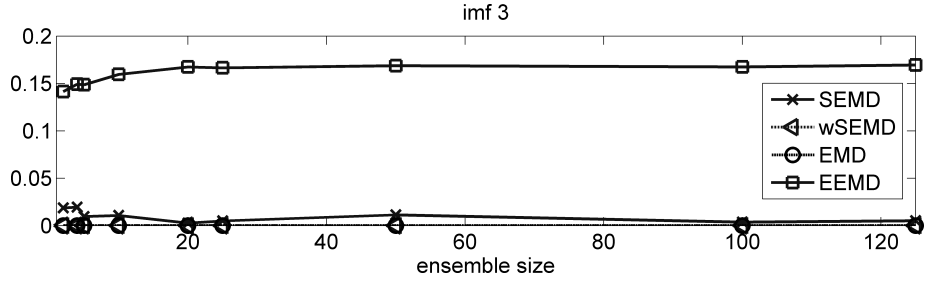

Fig. 7. Evolution of the mean of the absolute values of $m(t)$ for SIMF/IMF 3 obtained with SEMD, wSEMD, EMD, and EEMD of the toy data with respect to the ensemble size.

50 is utilized. The average value remains roughly stable, beginning at $E = 50$, which indicates that a decomposition with that parameter value is a good trade-off between computational load and reconstruction quality. In case of wSEMD, the mean value converges much faster than for SEMD and EEMD, respectively, thus reducing the computational effort drastically. For SIMF 3/IMF 3, the situation changes a bit (see Fig. 7). In this case, EEMD performs far worse than the other variants do. The SEMD algorithm produces some fluctuations with regard to the ensemble size. Again, wSEMD meets the first criterion as well as the classical EMD does.

3.2.3. *Number of extrema and zero crossings*

The difference between the number of extrema and zero crossings depending on the ensemble size is depicted in Figs. 8 and 9 for SIMF/IMF 1 and 3 of the toy example.

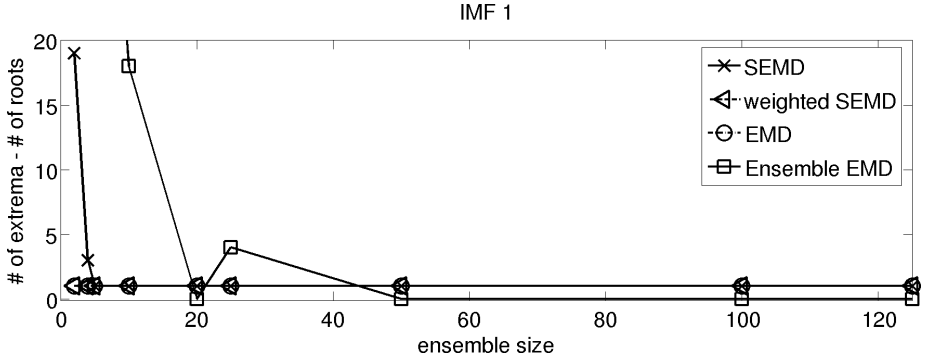

Fig. 8. Evolution of the difference between the number of extrema and zero crossings of IMF 1 obtained with SEMD, wSEMD, EMD, and EEMD of the toy data with respect to ensemble size.

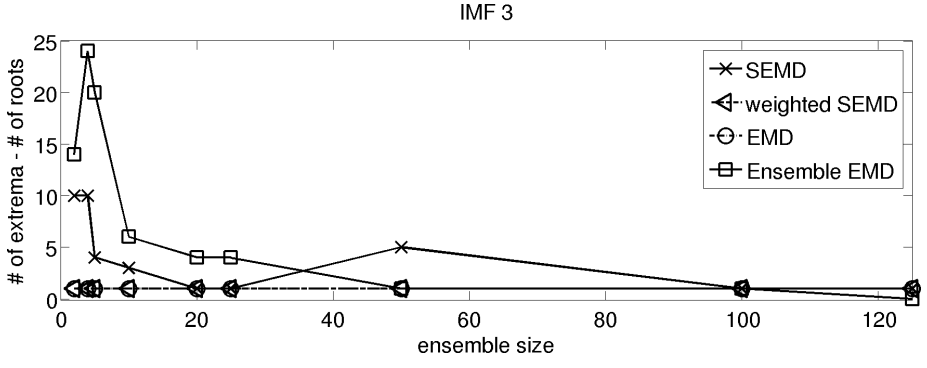

Fig. 9. Evolution of the difference between the number of extrema and zero crossings of IMF 3 obtained with SEMD, wSEMD, EMD, and EEMD of the toy data with respect to the ensemble size.

Whereas the EMD decomposition generally fulfills the second defining criterion for an IMF for the IMFs of the toy data example shown, EEMD fluctuates strongly for ensemble sizes <50. These high values for the difference originate from the potential ruggedness of the signals after the calculation of the average time series. SEMD and wSEMD, however, show a difference between the extrema and zero crossings larger than one only for small ensemble sizes. Especially, weighted SEMD meets the IMF requirement already for very small ensemble sizes E and is, therefore, to be preferred. Taking all discussed properties into account, one can conclude that the IMF constraints are very well satisfied by the extracted SIMFs regardless whether SEMD or wSEMD is employed.

3.2.4. *Varying step size and window size*

The following simulations investigate the impact of window size on the estimated sliding residuum as well as on the reconstruction quality of the SIMFs. Note that the number of IMFs to be extracted is fixed to $\lfloor j \rfloor = \log_2(m)$ where m designates the window size. This assures an identical number of extracted IMFs in every segment that is necessary for the construction of appropriate SIMFs. Furthermore, the frequencies of the underlying component signals have been chosen sufficiently different to avoid problems with resolution or mode mixing. The decomposition has been performed for all step sizes $k = 2, \ldots, 1,250$ separately. The latter always corresponded to a factor of the chosen window size used for the SEMD. The quality of the decomposition has been estimated for the three oscillatory components and the residuum in the following way:

$$Q = \frac{1}{N} \sum_{t=1}^{N} |s_i(t) - x_i(t)|^p, \tag{10}$$

where $s_i(t)$ denote the original signal components and $x_i(t)$ denote their corresponding SIMFs and the sliding residuum, respectively. Using $p = 1$ results in an average error, while $p = 2$ provides a mean squared error (MSE) measure. The latter will be used throughout the further analysis. Figure 10 shows the mean square error of component 1–3 and the residuum as function of the ensemble size.

With increasing ensemble size or decreasing step size, respectively, the reconstruction quality improves. Starting with an ensemble size of about $E = 50$ estimates, the MSE stays roughly constant. Therefore, the results show that for any practical application again an ensemble size of about $E = 50$ is a good trade-off between reconstruction quality and computational load. As seen before, in all cases, wSEMD components converge much faster than the SEMD components do. Using wSEMD, an ensemble size of about $E = 25$ already produces stable results.

In the following, we studied the influence of the window size on the reconstruction quality. The decomposition was applied for different segment sizes and a constant ensemble size $E = 50$. Figure 11 shows the resulting reconstruction quality of components 1–3 and the sliding residuum as a function of the segment size.

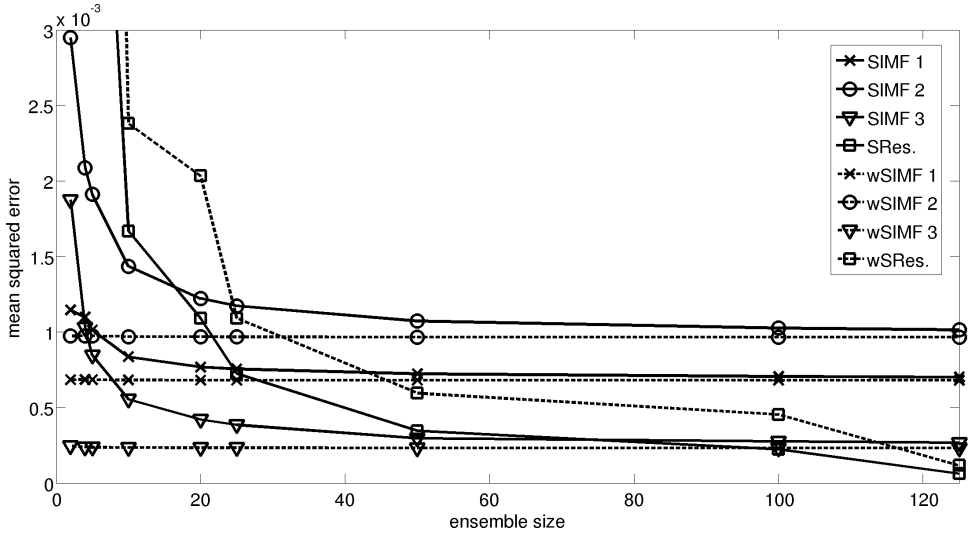

Fig. 10. Reconstruction error generated by SEMD/wSEMD for components 1–4 of the toy data as function of the ensemble size with segment size $m = 2{,}500$. Associated SIMFs/wSIMFs are labeled by identical markers.

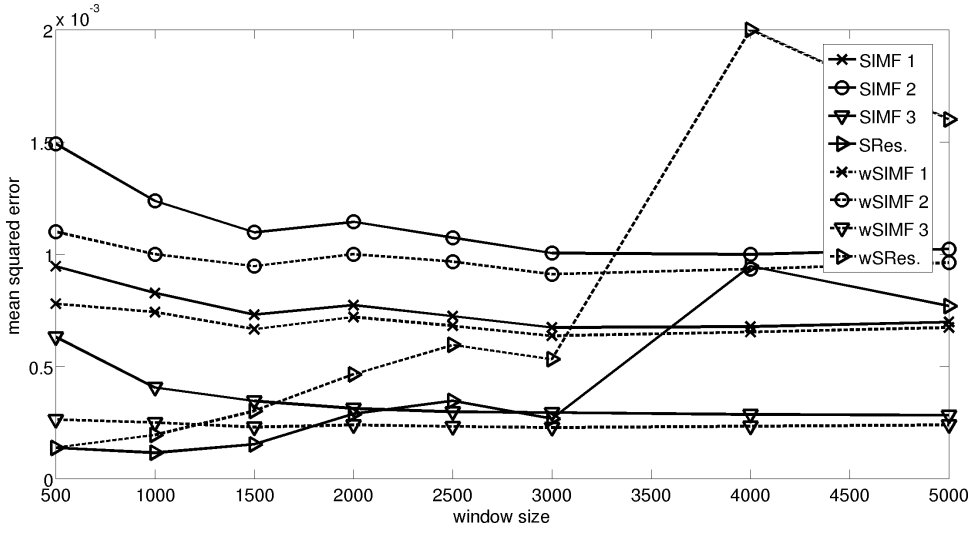

Fig. 11. Reconstruction error generated by SEMD/wSEMD for components 1–4 of the toy data as function of the window size with ensemble size $E = 50$. Associated SIMFs/wSIMFs are labeled by identical markers.

Especially for a window size of $m = 500$ and $m = 1{,}000$, the MSE is higher than for larger segment sizes. However, considering an absolute error value of at most MSE $= 0.0015$, the reconstruction still can be considered good. With increasing window size, the reconstruction error for the various underlying signal components

decreases, which also holds for all other number of estimates tested. Supposing that the artifacts caused by the boundary conditions have an almost constant penetration depth; for larger window sizes, the percentage of corrupted estimates naturally decreases. This effect may lead to a better reconstruction when using a larger window size. Again the wSEMD components 1–3 show lower errors and a faster convergence compared to SEMD. However, the reconstruction error of the sliding residuum increases with increasing window size. The MSE of the sliding residuum, as obtained by an SEMD/wSEMD decomposition, fluctuates strongly. This is because the final signal component resulting from a decomposition with SEMD does, after averaging over all suggestions for the data points, not necessarily resemble a smooth line. In the following, we will look a bit closer to this phenomenon.

3.2.5. *Segment size and periodic components of the sliding residuum*

The residuum of SEMD and wSEMD may contain periodic components if the periodicity is much larger than the selected window size. Components with a periodicity much smaller than the window size are extracted as respective IMFs. To evaluate the behavior of SEMD in an intermediate range of periodicities, a toy signal $\sin(2\pi \cdot x)(\Delta x = 0.0005)$ consisting of a sinusoid with a period of $T = 2{,}000$ data points and i.i.d. noise with an amplitude corresponding to 10% of the maximal amplitude of the sinusoid is decomposed with SEMD. Different segment sizes $m = 200, \ldots, 5{,}000$ were considered, whereas the ensemble size $E = 50$ was kept constant, and the central 26,000 data points (of 40,000 originally) were considered for the analysis. Eventually, the MSE of the residuum compared to the sine function was computed as can be seen in Fig. 12.

With increasing window size, the MSE increases discontinuously, because the amplitude of the sine function decreases as it is split up into the sliding residuum and an SIMF. The sinusoid resides entirely in the sliding residuum for window sizes

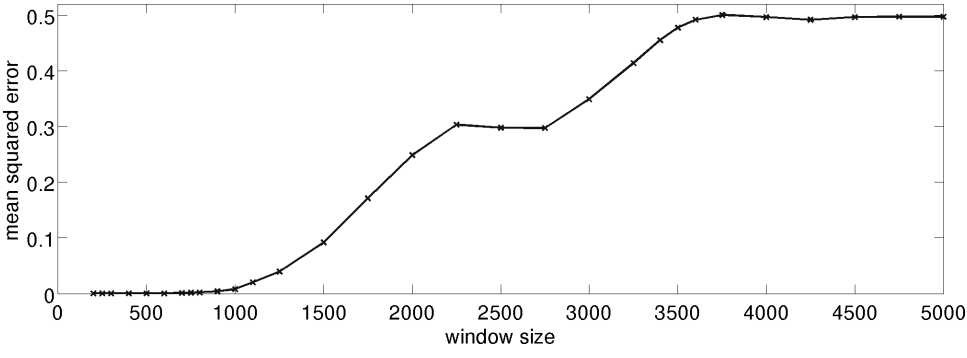

Fig. 12. MSE of the sliding residuum compared to the sinusoidal toy data as a function of the window size. The number of estimates was $E = 50$.

$m \leq 1{,}000$, corresponding to $m \leq 0.5 \cdot T$. The sinusoidal component is recovered completely in an SIMF for ca. $m \geq 3{,}500$, corresponding to $m \geq 1.75 \cdot T$. Depending on which oscillatory components of the original signal are supposed to appear in SIMFs, an appropriate window size has to be chosen when applying SEMD.

3.3. *Performance evaluation of SEMD and wSEMD*

In order to be able to assess the performance of SEMD and wSEMD, both systems were compared to the existing versions of EMD. Again the toy example consisting of a sawtooth wave, a sinusoid, a cosine function with a time-dependent frequency, and a monotonous trend (see Fig. 5) was used for demonstration purposes. The described time series was then decomposed with SEMD/wSEMD employing different window sizes (m = 500, 1,000, 1,500, 2,000, 2,500, 3,000, 4,000, and 5,000) as well as step sizes, so that the ensemble of estimates of each resulting data point remained constant at $E = 50$. Figures 13–16 show the reconstruction error of components 1–4 of the toy example reconstructed with SEMD/wSEMD in comparison to the decomposition with plain EMD. Depending on the window size, the summed up MSE is depicted.

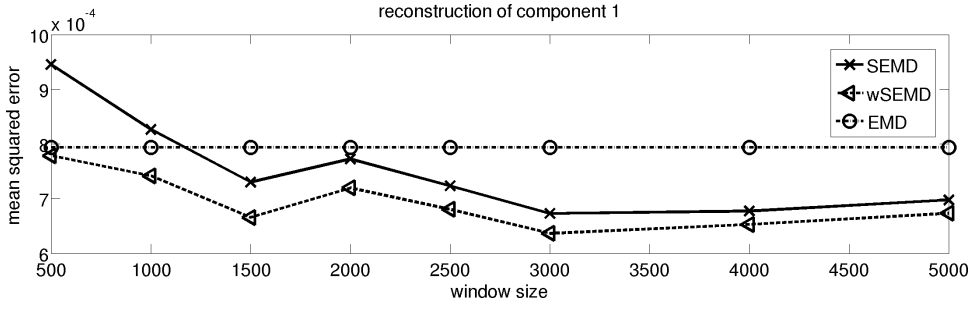

Fig. 13. Reconstruction error for component 1 of the toy data after the decomposition with SEMD, wSEMD, and EMD as a function of window size.

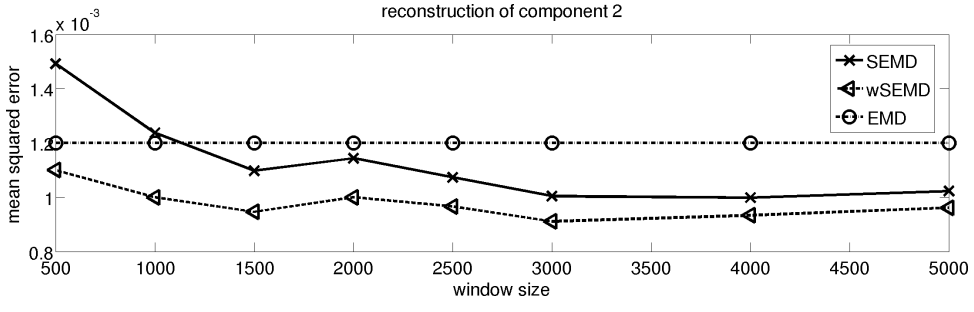

Fig. 14. Reconstruction error for component 2 of the toy data after the decomposition with SEMD, wSEMD, and EMD as a function of window size.

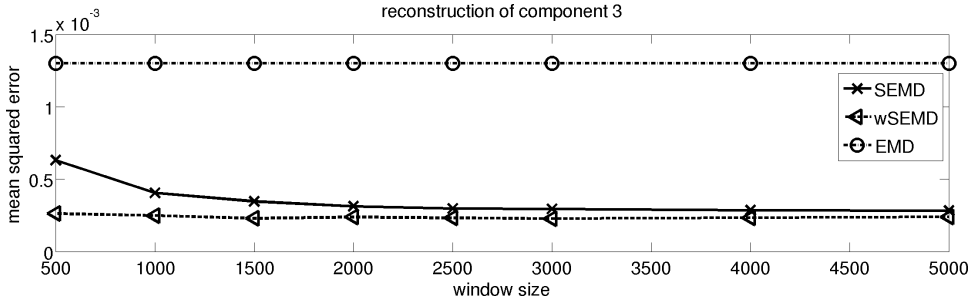

Fig. 15. Reconstruction error for component 3 of the toy data after the decomposition with SEMD, wSEMD, and EMD as a function of window size.

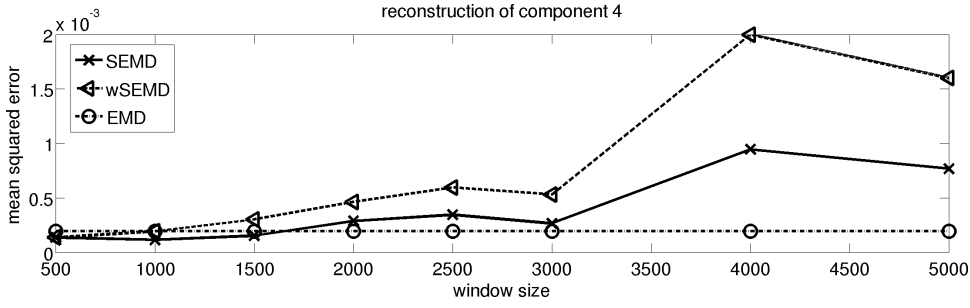

Fig. 16. Reconstruction error for component 4 of the toy data after the decomposition with SEMD, wSEMD, and EMD as a function of window size.

For SIMFs 1–3, the reconstruction error is generally slightly smaller compared to IMFs when the window size is larger than 1,500 and the wSEMD algorithm shows a faster convergence with respect to the window size. Consequently, the use of very small window sizes is not recommended. As already discussed above, when looking at the sliding residuum (see Fig. 16), for small window sizes ($m < 1,500$), the reconstruction errors produced by SEMD/wSEMD are comparable to the ones of EMD; but, with rising window size, the reconstruction errors grow and become more irregular with respect to the window size. Nevertheless, the resulting errors are very small regardless whether SEMD or wSEMD is applied.

As pointed out before, an on-line version of EMD was shortly mentioned by Flandrin (2009). Therefore, SEMD/wSEMD is compared to this on-line EMD as well. Furthermore, because of the averaging operation, SEMD bears a strong resemblance to EEMD. Thus, also these two methods are compared via their resulting MSEs. Figure 17 shows the sum of the reconstruction errors of all four components of the toy example decomposed with EMD, wSEMD, SEMD, on-line EMD, and EEMD with 50 iterations. The latter number was chosen for EEMD, as the ensemble of estimates for one component decomposed with SEMD/wSEMD had a size $E = 50$ as well.

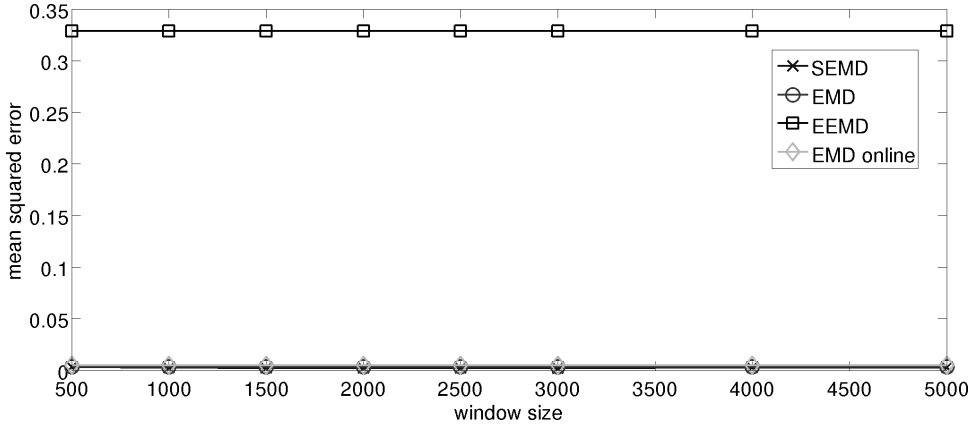

Fig. 17. Summed up reconstruction error of all components obtained with SEMD, EMD, EEMD, and on-line EMD as a function of window size.

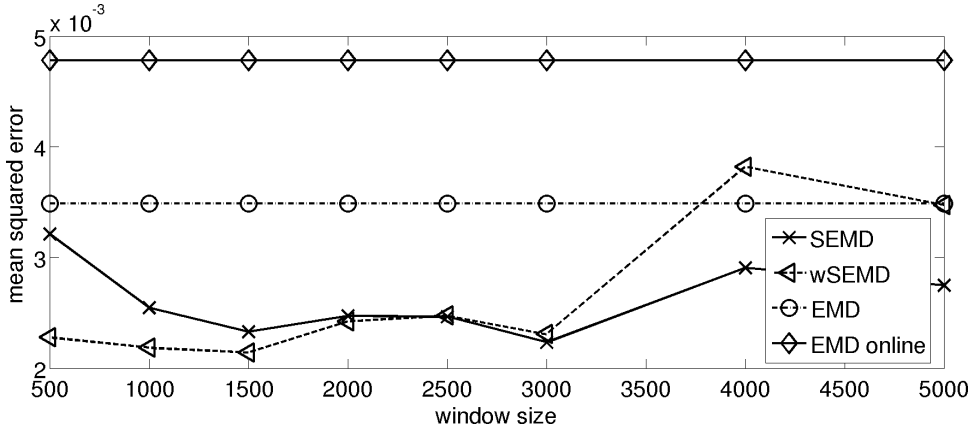

Fig. 18. Summed up reconstruction error of all components obtained with wSEMD, SEMD, EMD, and on-line EMD as a function of window size.

As the reconstruction with EEMD bore a huge amount of mode mixing, the reconstruction error was large and any serious comparison seemed hardly possible. Therefore, Fig. 18 shows the reconstruction quality of the other three methods separately and in more detail.

SEMD/wSEMD clearly outperforms EMD and on-line EMD yielding a much smaller reconstruction error. Note that better results are even obtained with plain EMD compared to on-line EMD. With an ensemble size of only $E = 50$ estimates, SEMD/wSEMD performs the most accurate decomposition of all tested methods and represents a high-quality data analysis. Additionally, it is a true on-line method and constitutes a more robust and more sophisticated tool than on-line EMD.

4. Conclusion

The newly proposed algorithms SEMD and wSEMD proof to be very performing when compared to diverse extensions of EMD and yield a decomposition well in accord with standard EMD. Both methods fulfill all IMF criteria much like the standard EMD algorithm does. Taking the computational effort into account, wSEMD yields superior results because it allows to reduce the ensemble size drastically when compared to SEMD. The window size of SEMD/wSEMD offers a parameter to control which periodic component of the signal should occur in the sliding residuum and which not. Therefore, this parameter cannot be chosen completely arbitrary if the residuum is to fulfill particular requirements. Additionally, computational time depends strongly on window size and step size, which constrains the choice of these parameters in practical applications. Hence, further investigations are currently under way in our laboratory (see also [Zeiler *et al.* (2010, 2011)] for some preliminary investigation to identify an optimal set of parameters for good reconstruction quality and a flexible handling of the window size. SEMD and wSEMD offer the additional advantage of being true *on-line* algorithms that are able handling time series of arbitrary length with bearable computational costs. They are both as flexible as standard EMD in detrending applications, and allow extracting the stationary part of originally nonstationary time series data.

References

Faltermeier, R., Zeiler, A., Keck, I. R., Tomé, A. M., Brawanski, A. and Lang, E. W. (2010). Sliding empirical mode decomposition. in *WCCI-IJCNN2010*.

Flandrin, P. (2009). http://perso.ens-lyon.fr/patrick.flandrin/software2.html.

Flandrin, P., Gonçalvès, P. and Rilling, G. (2005). EMD equivalent filter banks: from interpretation to application. *Hilbert-Huang Transform: Introduction and Application*. eds. N. Huang and S. Shen, World Scientific, Singapore, pp. 67–87.

Huang, N. E., Shen, Z., Long, S. R., Wu, M. L., Shih, H. H., Zheng, Q., Yen, N. C., Tung, C. C. and Liu, H. H. (1998). The empirical mode decomposition and Hilbert spectrum for nonlinear and nonstationary time series analysis. *Proc. R. Soc. Lond. A*, **454**: 903–995.

Jánosi, I. M. and Müller, R. (2005). Empirical mode decomposition and correlation properties of long daily ozone records. *Phys. Rev. E*, **71**: 056126.

Rilling, G., Flandrin, P. and Goncalès, P. (2003). On empirical mode decomposition and its algorithms, *Proceedings of the 6th IEEE-EURASIP Workshop on Nonlinear Signal and Image Processing*. Grado, Italy.

Wu, Z. and Huang, N. (2004). A study of the characteristics of white noise using the empirical mode decomposition method. *Proc. R. Soc. Lon. A* **460**: 1597–1611.

Wu, Z. and Huang, N. (2009). Ensemble empirical mode decomposition: A noise assisted data analysis method. *Adv. Adapt. Data Anal.*, **1**: 1–41.

Zeiler, A., Faltermeier, R., Böhm, M., Keck, I. R., Tomé, A. M., Puntonet, C. G., Brawanski, A. and Lang, E. W. (2011). *Empirical Mode Decomposition Techniques for Biomedical Time Series Analysis*. Bentham Science Publishers Ltd.

Zeiler, A., Faltermeier, R., Keck, I. R., Tomé, A. M., Brawanski, A., Puntonet, C. G. and Lang, E. W. (2010). Sliding empirical mode decomposition for online analysis of biomedical time series. *Proceeding of IEEE EMBC 2010*, IEEE.